Physics of Fluids

Four-temperature kinetic model for CO_2 vibrational relaxation

Cite as: Phys. Fluids **33**, 016103 (2021); https://doi.org/10.1063/5.0035171
Submitted: 26 October 2020 . Accepted: 16 December 2020 . Published Online: 06 January 2021

A. Kosareva, O. Kunova, E. Kustova, and E. Nagnibeda

Physics of Fluids ARTICLE scitation.org/journal/phf

Four-temperature kinetic model for CO_2 vibrational relaxation

Cite as: Phys. Fluids 33, 016103 (2021); doi: 10.1063/5.0035171
Submitted: 26 October 2020 • Accepted: 16 December 2020 •
Published Online: 6 January 2021

A. Kosareva,[a] O. Kunova,[b] E. Kustova,[c] and E. Nagnibeda[d]

AFFILIATIONS

Saint-Petersburg State University, Department of Mathematics and Mechanics, 7/9 Universitetskaya nab., St. Petersburg 199034, Russia

[a]Electronic mail: kos-hellen@yandex.ru
[b]Electronic mail: o.kunova@spbu.ru
[c]Author to whom correspondence should be addressed: e.kustova@spbu.ru
[d]Electronic mail: e_nagnibeda@mail.ru

ABSTRACT

A four-temperature kinetic-theory approach for modeling vibrationally non-equilibrium carbon dioxide flows is developed. The model takes into account all kinds of vibrational–translational energy transitions and inter-mode vibrational energy exchange between symmetric, bending, and asymmetric CO_2 modes. The key feature of the model is using the averaged state-resolved relaxation rates instead of conventional Landau–Teller expressions. Spatially homogeneous CO_2 vibrational relaxation is studied using the state-to-state, new four-temperature and commonly used three-temperature models. Excellent agreement between four-temperature and state-to-state solutions is found, whereas using the three-temperature model with the Landau–Teller production rates leads to significant loss of accuracy. Numerical efficiency of various approaches is discussed as well as the ways for its improvement.

I. INTRODUCTION

Modeling non-equilibrium vibrational kinetics in CO_2 flows is important for many applications, in particular for the prediction of flow parameters near spacecrafts entering the Mars and Venus atmospheres, in environmental problems, and in low-temperature plasma technologies. Models of various complexities were developed in both kinetic and continuum approaches for different scalings of characteristic times of vibrational energy transitions and chemical reactions.[1–8] The most accurate state-to-state flow description is based on the solution of the master equations for the level populations of three CO_2 vibrational modes coupled to fluid-dynamic equations.[3,9] There are, however, several challenges in practical implementation of this approach. The first one is the necessity to solve a huge number of equations for vibrational–chemical kinetics for the level populations of symmetric, bending, and asymmetric CO_2 modes coupled to conservation equations. This is particularly complicated for viscous flow simulations since it requires computation of state-resolved transport coefficients. Another difficulty is the calculation of hundreds of thousands of state-dependent rate coefficients for vibrational energy transitions and chemical reactions and the absence of reliable data for their assessment except old experiments[10,11] and a few quasi-classical trajectory calculations.[12] Theoretical models for the rate coefficients[13–16] are commonly adjusted using these experimental data.

The state-to-state approach was used in Refs. 3 and 17–23 for a variety of problems: spatially homogeneous relaxation, stagnation line flows, and low-temperature plasma applications. Various sets of vibrational levels were used, from the complete set of several thousands states[23] to the reduced set of about 25 levels.[17] Many interesting effects were discovered in the frame of these simulations. However, the use of the state-to-state approach in real fluid-dynamic simulations is not possible at the present time, and the development of reduced-order models is of crucial importance. At the same time, state-to-state solutions based on the full set of vibrational states and complete kinetic schemes may serve as benchmarks for the reduced-order model assessment.

Multi-temperature models for CO_2 kinetics can be developed if the rates of various vibrational energy transitions differ by at least one order of magnitude under similar temperature conditions. Thus,

a three-temperature description of CO_2 relaxation is based on introducing two vibrational temperatures T_{12} and T_3, taking into account rapid vibrational energy exchanges within modes and between symmetric and bending CO_2 modes due to the Fermi resonance. Expressions for CO_2 vibrational level populations depending on T_{12} and T_3 are obtained empirically[24] and using the kinetic theory.[2]

A more simple two-temperature CO_2 relaxation model[10] is derived under the assumption of rapid inter-mode vibrational energy exchange compared to vibrational–translational (VT) relaxation within modes; this allows introducing the overall CO_2 vibrational temperature $T_V = T_{12} = T_3$.

In our recent work,[23] a comparison of full state-to-state and several multi-temperature solutions was carried out for spatially homogeneous relaxation under various initial conditions. Single-component carbon dioxide without chemical reactions was considered for the sake of simplicity. It was shown that the two-temperature model provides poor agreement with the state-to-state solution; the three-temperature model works much better, especially if the vibrational energy production rates are calculated by averaging the corresponding state-resolved rates. Yet, there is a discrepancy between three-temperature and state-to-state solutions, which can attributed to the importance of VT_1 transitions in the symmetric mode and VV_{1-2} exchange between the symmetric and bending modes. The latter processes cannot be accurately described in the frame of the three-temperature model.

The objective of the present study is to develop and assess a new four-temperature model. The distinct features of the model are as follows: (1) it does not assume coupling of symmetric and bending vibrations due to VV_{1-2} energy transitions on the microscopic time scale and therefore allows introducing different temperatures for all CO_2 vibrational modes; (2) it uses averaged state-resolved relaxation rates instead of conventional Landau–Teller expressions; this makes the new model suitable for arbitrary deviations from thermal equilibrium and considerably extends the range of applicability for multi-temperature simulations.

This paper is organized as follows: first, we briefly remind the peculiarities of state-to-state and multi-temperature flow descriptions. Then, we derive the four-temperature distributions and corresponding governing equations; after that, we carry out the numerical study of space-homogeneous CO_2 relaxation in the four-temperature approximation and compare the results with those obtained using the three-temperature model for the same initial conditions. The vibrational energy production rates are calculated using both traditional Landau–Teller expressions and averaged state-dependent rates. To estimate the accuracy of two considered models, the results are compared with corresponding state-to-state solutions; thus, the ranges of validity for the reduced-order models are evaluated. Finally, the computational efficiency of different models is discussed.

II. THEORETICAL MODELS

Existence of three vibrational modes in CO_2 molecules and their interaction leads to multiple relaxation channels. In the present study, the following set of kinetic processes is considered:[3,23]

1. VT_m energy exchanges between translational energy and vibrational energy of the mth CO_2 mode (m = 1, 2, 3) as a result of the collision of two CO_2 molecules;
2. intermode VV_{1-2}, VV_{2-3}, VV_{1-2-3} exchanges inside one molecule;
3. intramode VV_m exchanges of vibrational quanta in each mth mode of the CO_2 molecule.

Basically, among VT processes, only VT_2 exchanges are taken into account since their rates are considerably higher than those of VT_1 and VT_3 exchange.[1] This assumption was assessed in Ref. 23, and it was shown that VT_1 transitions considerably affect the temperature evolution and, therefore, cannot be neglected. On the other hand, intramode VV_m exchanges, while being computationally expensive, do not alter the temperature distribution in the state-to-state simulations. Therefore, VV_m transitions are neglected in the state-resolved production terms. However, they are taken into account in the fast processes, when we develop multi-temperature models.

A. State-to-state model

The state-to-state flow description is well known in the literature and has to be applied under conditions of rapid translational–rotational and slow vibrational relaxation,[2]

$$\tau_{\mathrm{tr}} < \tau_{\mathrm{rot}} \ll \tau_{\mathrm{vibr}} \sim \theta. \tag{1}$$

Here, τ_{tr}, τ_{rot}, and τ_{vibr} are the mean times of translational, rotational, and vibrational relaxation and θ is the macroscopic relaxation time. In this case, all vibrational energy transitions are considered at the fluid-dynamic time scale, and populations of all vibrational states are treated as macroscopic flow variables together with density, velocity, and temperature.

Under condition Eq. (1), the set of governing equations describing CO_2 space-homogeneous vibrational relaxation contains the equations for vibrational level populations n_{i_1,i_2,i_3} and the energy conservation equation,[23]

$$\frac{dn_{i_1,i_2,i_3}}{dt} = R_{i_1,i_2,i_3} = \sum_{\gamma} R^{\gamma}_{i_1,i_2,i_3}, \tag{2}$$

$$\begin{aligned} &i_m = 0, \ldots, l_m, \quad m = 1, 2, 3, \\ &U = E_{\mathrm{tr}} + E_{\mathrm{rot}} + E_{\mathrm{vibr}} = const. \end{aligned} \tag{3}$$

Here, U is the gas energy per unit mass, whereas E_{tr}, E_{rot}, and E_{vibr} are the specific energies of translational, rotational, and vibrational degrees of freedom,

$$\rho E_{\mathrm{tr}} = \frac{3}{2} n k_B T, \tag{4}$$

$$\rho E_{\mathrm{rot}} = n k_B T, \tag{5}$$

$$\rho E_{\mathrm{vibr}} = \sum_{i_1,i_2,i_3} n_{i_1,i_2,i_3} \varepsilon_{i_1,i_2,i_3}, \tag{6}$$

where ρ is the gas density, n is the total number density, k_B is the Boltzmann constant, T is the gas temperature, and $\varepsilon_{i_1,i_2,i_3}$ is the vibrational energy of a molecule at the (i_1, i_2, i_3)th vibrational state. The vibrational energy of a CO_2 molecule was described on the basis of both the harmonic and anharmonic oscillator models[25] with $l_{1/2/3}$ = 30/61/17 and $l_{1/2/3}$ = 30/62/19, respectively. Thus, the set of coupled vibrational states located below dissociation energy, which

is used in our simulations, includes about 8000 and 6000 states for anharmonic and harmonic oscillators, correspondingly.

Production terms $R^{\gamma}_{i_1,i_2,i_3}$ in Eq. (2) describe the variation of vibrational level populations n_{i_1,i_2,i_3} due to all kinds of vibrational energy transitions (γ stands for VT_m, VV_m, and VV_{k-m} exchanges). The expressions for all $R^{\gamma}_{i_1,i_2,i_3}$ are given in Ref. 23. For the simulations, the rate coefficients of vibrational energy transitions are calculated using the SSH model,[13] which provides the complete set of required rate coefficients. Although the SSH model is rather approximate, it is sufficient for our purpose of reduced-order model assessment on the basis of the state-to-state solutions. To be self-consistent and avoid additional uncertainties, it is important to use the same model for the rate coefficients in the state-to-state and multi-temperature simulations.

The state-to-state approach was applied in many studies, both for high-temperature hypersonic flows[3,4,22] and low-temperature plasma applications.[17,18,26,27] Under high-temperature conditions, the model was assessed in Ref. 22 by comparison with the surface heat flux measured in Refs. 28 and 29; fairly good agreement between the calculated and measured heat fluxes was shown. Carbon dioxide infrared radiation under a non-equilibrium expansion was measured in Ref. 30, and highly complicated vibrational energy distribution in the expansion tube was found; possible shortcomings of the multi-temperature models and necessity for the state-to-state simulations are discussed. For low-temperature kinetics, the state-to-state model was validated in Ref. 27, where the time-dependent vibrational level populations were compared with experimental data obtained from time-resolved Fourier transform infrared spectroscopy; again, good agreement between the model predictions and the experimental results is found. Thus, it was confirmed that the state-to-state approach presents a detailed and accurate tool for strongly non-equilibrium flow simulations. This allows us to consider the state-to-state solutions as benchmark solutions for the assessment of reduced-order models.

B. Four-temperature approach

In this section, we develop a new four-temperature kinetic model based on the assumption that vibrational energy exchanges $\mathrm{VV_m}$ within each CO_2 mode ($m = 1, 2, 3$) proceed faster than other processes, whereas all VT and inter-mode transitions occur slowly. In this case, the relation for the characteristic times takes the form

$$\tau_{tr} < \tau_{rot} < \tau_{\mathrm{VV_m}} \ll \tau_{\mathrm{VV}_{1-2}} \sim \tau_{\mathrm{VT_m}} \sim \tau_{\mathrm{VV}_{2-3}} \sim \tau_{\mathrm{VV}_{1-2-3}} \sim \theta, \quad m = 1, 2, 3. \tag{7}$$

Such time scaling is commonly applied for diatomic species;[2] indeed, in diatomic molecules, the rates of VT transitions are much lower than those of VV exchanges. However, in carbon dioxide, the symmetric and bending modes are usually assumed connected through fast inter-mode VV_{1-2} transitions, which prevents introducing different temperatures for the first and second modes.

In kinetic theory, the macroscopic description of a non-equilibrium flow is derived starting from collision invariants of rapid processes.[2] The common invariants of any collision are the mass, momentum, and total energy of colliding particles. Under condition (7), the additional invariants of rapid processes for anharmonic oscillators are the numbers of vibrational quanta in each vibrational mode of the CO_2 molecule: i_1, i_2, and i_3. Such invariants were introduced by Treanor for diatomic gases;[31] in the present work, they are extended to polyatomic species. For harmonic oscillators, the additional invariants are the vibrational energies of the three CO_2 modes, which remain isolated during VV_m transitions.

For the above set of collision invariants, the corresponding set of fluid-dynamic variables includes the density, gas velocity, total specific energy, and additional variables, namely, specific numbers of vibrational quanta in each CO_2 mode,

$$\rho W_m = \sum_{i_1,i_2,i_3} i_m n_{i_1,i_2,i_3}, \quad m = 1, 2, 3. \tag{8}$$

Introducing the total specific energy U and specific numbers of vibrational quanta W_m as macroscopic flow variables is equivalent to introducing the gas temperature T and three vibrational temperatures of symmetric, bending, and asymmetric modes of CO_2 molecules T_1, T_2, and T_3. The vibrational distribution in this case represents the Treanor-like four-temperature distribution over vibrational levels,

$$n_{i_1,i_2,i_3} = \frac{n s_{i_1,i_2,i_3}}{Z^{\mathrm{vibr}}(T, T_1, T_2, T_3)} \times \exp\left(-\frac{\varepsilon_{i_1,i_2,i_3} - (i_1\varepsilon_{1,0,0} + i_2\varepsilon_{0,1,0} + i_3\varepsilon_{0,0,1})}{k_B T} - \frac{i_1\varepsilon_{1,0,0}}{k_B T_1} - \frac{i_2\varepsilon_{0,1,0}}{k_B T_2} - \frac{i_3\varepsilon_{0,0,1}}{k_B T_3}\right). \tag{9}$$

Here, $s_{i_1,i_2,i_3} = i_2 + 1$ is the vibrational statistical weight, and Z^{vibr} is the corresponding vibrational partition function,

$$Z^{\mathrm{vibr}}(T, T_1, T_2, T_3) = \sum_{i_1,i_2,i_3} s_{i_1,i_2,i_3} \times \exp\left(-\frac{\varepsilon_{i_1,i_2,i_3} - (i_1\varepsilon_{1,0,0} + i_2\varepsilon_{0,1,0} + i_3\varepsilon_{0,0,1})}{k_B T} - \frac{i_1\varepsilon_{1,0,0}}{k_B T_1} - \frac{i_2\varepsilon_{0,1,0}}{k_B T_2} - \frac{i_3\varepsilon_{0,0,1}}{k_B T_3}\right). \tag{10}$$

For such distributions, the specific energy and numbers of quanta are functions of four temperatures,

$$U = U(T, T_1, T_2, T_3), \quad W_m = W_m(T, T_1, T_2, T_3), \quad m = 1, 2, 3. \tag{11}$$

In the four-temperature approach, the set of equations describing spatially homogeneous relaxation contains equations for specific numbers of quanta W_1, W_2, and W_3 coupled to the total energy conservation equation,

$$\rho \frac{dW_1}{dt} = \sum_{i_1,i_2,i_3} i_1 R_{i_1,i_2,i_3}, \tag{12}$$

$$\rho \frac{dW_2}{dt} = \sum_{i_1,i_2,i_3} i_2 R_{i_1,i_2,i_3}, \tag{13}$$

$$\rho \frac{dW_3}{dt} = \sum_{i_1,i_2,i_3} i_3 R_{i_1,i_2,i_3}, \tag{14}$$

$$U = E_{tr} + E_{rot} + E_{vibr} = const. \tag{15}$$

The right-hand sides of Eqs. (12)–(14) are calculated by averaging the state-resolved production rates R_{i_1,i_2,i_3} for slow processes chosen according to Eq. (7). In the present case, VV_m transitions are not included to the summation since their rates are higher than those for other processes. Note that the proposed technique is rather accurate although computationally demanding. Usually in multi-temperature models, the energy production rates are calculated according to the Landau–Teller expressions based on the corresponding relaxation times (see Subsection II C). However, in the present model, the absence of experimental data on the VT relaxation times in the symmetric and asymmetric modes as well as those for VV_{1-2} transitions does not allow using the Landau–Teller approach.

For harmonic oscillators, the problem is simplified. First, the vibrational distributions take the form of the Boltzmann distribution,

$$n_{i_1,i_2,i_3} = \frac{n s_{i_1,i_2,i_3}}{Z^{\text{vibr}}(T_1,T_2,T_3)} \exp\left(-\frac{i_1\varepsilon_{1,0,0}}{k_B T_1} - \frac{i_2\varepsilon_{0,1,0}}{k_B T_2} - \frac{i_3\varepsilon_{0,0,1}}{k_B T_3}\right), \quad (16)$$

with

$$\begin{aligned} Z^{\text{vibr}}(T_1,T_2,T_3) &= Z_1(T_1)Z_2(T_2)Z_3(T_3) \\ &= \sum_{i_1} \exp\left(-\frac{i_1\varepsilon_{1,0,0}}{k_B T_1}\right) \sum_{i_2} (i_2+1) \exp\left(-\frac{i_2\varepsilon_{0,1,0}}{k_B T_2}\right) \\ &\quad \times \sum_{i_3} \exp\left(-\frac{i_3\varepsilon_{0,0,1}}{k_B T_3}\right). \end{aligned} \quad (17)$$

The specific numbers of vibrational quanta in each mode depend on the corresponding tempeature,

$$\rho W_m(T_m) = \frac{n}{Z_m} \sum_{i_m} i_m s_m \exp\left(-\frac{i_m\varepsilon_m}{k_B T_m}\right), \quad m = 1,2,3. \quad (18)$$

ε_m is the energy of the first state in the corresponding mode ($\varepsilon_{1,0,0}$, $\varepsilon_{0,1,0}$, or $\varepsilon_{0,0,1}$), $s_1 = s_3 = 1$, and $s_2 = i_2 + 1$. The total specific energy still depends on the four temperatures.

It is worth mentioning that the Treanor-like vibrational distributions (9) are valid for the vibrational levels located below the state where the distribution minimum is achieved. For the highly excited gas, distributions (9), after attaining the minimum, increase with the vibrational state; however, increasing branches are not observed in experiments, and for the macroscopic gas description, the distributions are cut at the minimum values. For diatomic species, the minimum of the Treanor distribution is calculated analytically. For polyatomic species, coupling of vibrational modes does not allow for an explicit calculation of the minimum. Therefore, in the present study, we use the Treanor distribution only for the cases with $T_m < T$ to avoid unphysical results.

Applying the generalized Chapman–Enskog method,[2] one can write the set of four-temperature governing equations in the viscous flow approximation and derive the expressions for the transport terms and transport coefficients. This formalism is well established in kinetic theory; for CO_2, it was developed in Refs. 1 and 32. Linear transport systems for the transport coefficient computation depend on the collision integrals and have to be solved numerically. In multi-temperature models, the cost of transport coefficient calculation is significantly lower than in the state-to-state approach. The evaluation of the transport terms is, however, beyond the scope of the present study.

The four-temperature model presented above is the most detailed among multi-temperature descriptions of CO_2 flows since it takes into account VT transitions in all modes as well as all inter-mode VV transitions. Until now, it has not been used for flow simulations due to the absence of VT_1, VT_3, and VV_{1-2} relaxation times. Our approach based on the averaged state-resolved production rates allows implementing this model to the computational fluid dynamics (CFD). An alternative simplified description is discussed in Subsection II C.

C. Three-temperature approach

In the three-temperature approach used in many studies (see, for instance, Refs. 1, 33, and 34), the common vibrational temperature T_{12} of the combined symmetric-bending mode is introduced instead of vibrational temperatures T_1 and T_2. This model is based on the close values of the symmetric mode vibrational frequency and the doubled frequency of the bending mode; such a relation leads to rapid near-resonant VV_{1-2} vibrational energy exchange between these modes. The vibrational level populations are expressed as follows:

$$\begin{aligned} n_{i_1,i_2,i_3} &= \frac{n s_{i_1,i_2,i_3}}{Z^{vibr}(T,T_{12},T_3)} \\ &\quad \times \exp\left(-\frac{\varepsilon_{i_1,i_2,i_3} - (i_1\varepsilon_{1,0,0} + i_2\varepsilon_{0,1,0} + i_3\varepsilon_{0,0,1})}{k_B T}\right. \\ &\quad \left. -\frac{i_1\varepsilon_{1,0,0} + i_2\varepsilon_{0,1,0}}{k_B T_{12}} - \frac{i_3\varepsilon_{0,0,1}}{k_B T_3}\right). \end{aligned} \quad (19)$$

$Z^{vibr}(T, T_{12}, T_3)$ is the corresponding vibrational partition function. In this case, the set of equations for the fluid-dynamic variables n, T, T_{12}, and T_3 for space-homogeneous vibrational CO_2 relaxation takes the form[34]

$$\rho\frac{dW_{12}}{dt} = R_{12} = \sum_{\gamma} \sum_{i_1,i_2,i_3} (2i_1 + i_2) R^{\gamma}_{i_1,i_2,i_3}, \quad (20)$$

$$\rho\frac{dW_3}{dt} = R_3 = \sum_{\gamma} \sum_{i_1,i_2,i_3} i_3 R^{\gamma}_{i_1,i_2,i_3}, \quad (21)$$

$$U = E_{tr} + E_{rot} + E_{vibr} = const, \quad (22)$$

and γ stands for the slow processes VT_2, VV_{2-3}, and VV_{1-2-3}. Note that VT_1 and VV_{1-2} transitions cannot be included to Eqs. (20) and (21).

The relaxation rates in these equations can be calculated using the averaged state-resolved production terms $R^{\gamma}_{i_1,i_2,i_3}$ or, alternatively, using the approximate Landau–Teller formulation based on the relaxation times τ_γ of different processes,[33,35]

$$R_{12} = \sum_{\gamma} \rho \frac{W^{eq}_{12}(T) - W_{12}(T,T_{12})}{\tau_\gamma}, \quad (23)$$

$$R_3 = \sum_{\gamma} \rho \frac{W^{eq}_{3}(T) - W_{3}(T,T_3)}{\tau_\gamma}. \quad (24)$$

Here, W^{eq}_{12}, W^{eq}_{3} are equilibrium values of corresponding specific numbers of quanta. In the present study, the characteristic relaxation times of energy exchanges are calculated using the data of Ref. 36.

It is worth mentioning that the three-temperature model with the averaged state-resolved production rates coupled to a line by line model for CO_2 vibrational non-equilibrium radiation was applied in Ref. 37; a nozzle expansion and a plume of a high altitude solid propellant rocket engine were studied in this approach; strong deviations from the results obtained in the local thermal equilibrium approach were emphasized. In diatomic species, the multi-temperature approach based on averaging the state-resolved reaction rates was used in Refs. 38 and 39; good agreement with experimental data and state-to-state simulations was shown for shock heated flows.

III. RESULTS AND DISCUSSION

In this section, we present the results obtained in the four-temperature (4T) approximation and show the comparison with the solutions found in the state-to-state (STS) approach[23] and with the use of the three-temperature (3T) model.

A. Assessment of multi-temperature models accuracy

First, we consider two test cases with the initial conditions, which do not distinguish vibrational temperatures of different modes:

C1: $T^{(0)} = 3000$ K, $T_V^{(0)} = 1000$ K;
C2: $T^{(0)} = 1000$ K, $T_V^{(0)} = 3000$ K.

Here, $T_V^{(0)}$ is the overall initial vibrational temperature, common for all CO_2 modes. The initial pressure is $p^{(0)} = 100$ Pa. The first case is typical for high-temperature shock heated flows, whereas the second one characterizes low-temperature expanding flows. In the state-to-state approach, the initial population of vibrational levels is specified by the Boltzmann distribution with the vibrational temperature $T_V^{(0)}$.

In Fig. 1, the gas temperature variation is shown as a function of time for the state-to-state, four-temperature, and three-temperature approaches for the first test case, $T^{(0)} > T_V^{(0)}$. The results are obtained using both the harmonic [Fig. 1 (top)] and anharmonic [Fig. 1 (bottom)] models for molecular vibrations. State-dependent rate coefficients of all vibrational energy transitions are calculated using the SSH theory.[13] In the four-temperature approach, the rate coefficients of transitions are found averaging the state-resolved coefficients over four-temperature vibrational distributions (9) and (16). Three-temperature rate coefficients are calculated using two ways: (1) averaging state-dependent coefficients over three-temperature distributions and (2) using Landau–Teller formulas (23) and (24).[23,33] One can observe very close agreement of the gas temperatures obtained in the four-temperature approach and using the most accurate state-to-state description during the entire relaxation process. The difference does not exceed 3%. The three-temperature solution noticeably deviates from the benchmark state-to-state solution. When the averaged STS rate coefficients are used for the calculation of the energy production rates, agreement is fairly good for the first several microseconds and for $t > 100$ μs. The maximum discrepancy is found for the time about 10 μs; in this time range, the 3T model underestimates the gas temperature. Using the Landau–Teller model yields rather poor agreement with the STS solution in the entire computational domain. It can be noticed that for the considered test case, very close values of the gas temperature are obtained with the use of both the harmonic and anharmonic oscillator models.

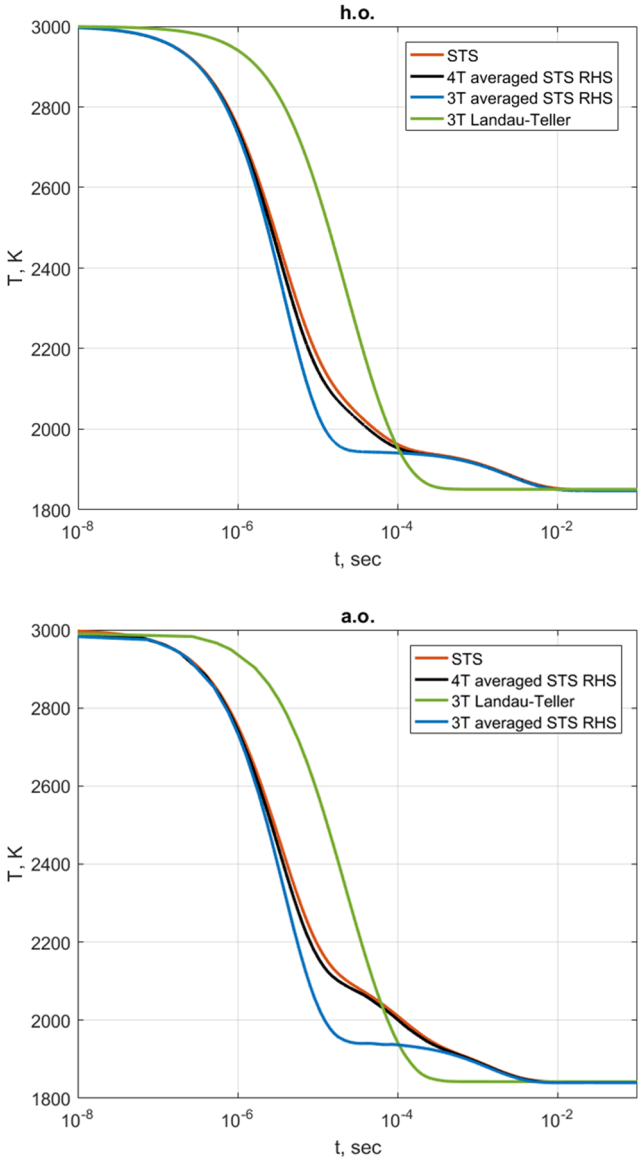

FIG. 1. Evolution of the gas temperature for test case C1 with $T^{(0)} > T_V^{(0)}$. Vibrational energy model: harmonic oscillator (h.o., top panel) and anharmonic oscillator (a.o., bottom panel).

The results for the second test case, C2, are presented in Fig. 2. The harmonic oscillator model is used in these simulations since in CO_2, the minimum of the Treanor distribution cannot be correctly specified. Again, agreement between the 4T and STS solutions is excellent. The 3T model with the averaged STS transition rates works rather well in the beginning of the relaxation process

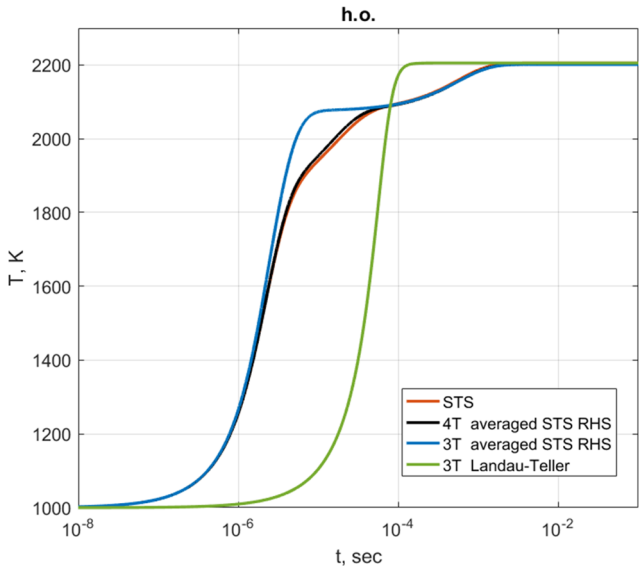

FIG. 2. Evolution of the gas temperature for test case C2 with $T^{(0)} < T_V^{(0)}$. Harmonic oscillator model.

and for $t > 50$ μs–60 μs; at the intermediate time interval, it overpredicts the gas temperature. Using the simplified Landau–Teller formulation yields significant loss of accuracy, overestimated incubation time of vibrational relaxation, and faster approaching to the equilibrium.

The time distribution of the gas temperature and mode vibrational temperatures T_1, T_2, and T_3 obtained in the four-temperature approach for anharmonic oscillators is presented in Fig. 3. The plots show the specific features of the relaxation process under different conditions: for case C1 described above and also for the higher initial temperature, $T^{(0)} = 6000$ K. It should be noted that for the high initial gas temperature (Fig. 3, bottom panel), the dissociation may have a strong effect; however, in the present paper, our focus is on the vibrational relaxation; therefore, we do not account for dissociation. One can see (Fig. 3, top panel) that the relaxation of each mode is mainly driven by VT processes, and the order in which T_m begin to increase is determined by the ratio between the rates of VT processes. Whereas for the lower temperature inter-mode VV exchange weakly affects the relaxation, by increasing the initial gas temperature, these transitions and, especially, the VV_{1-2} exchange become important; the profiles of vibrational temperatures T_1, T_2 become closer at the very beginning of the relaxation. The same trend is found for solutions using the harmonic oscillator model and initially excited vibrational modes (case C2). It is interesting that in many earlier works,[1,40] it is commonly assumed that the temperatures of symmetric and bending modes equalize very fast, which provides the basis for the 3T model. The present analysis shows that this assumption has to be thoroughly assessed. It is also worth noting that using another model for the transition rate coefficients (for instance, the FHO model) may alter this conclusion; we plan to check this in our future studies. Nevertheless, in many cases, the 3T model still yields rather realistic gas temperature profiles; this is discussed below.

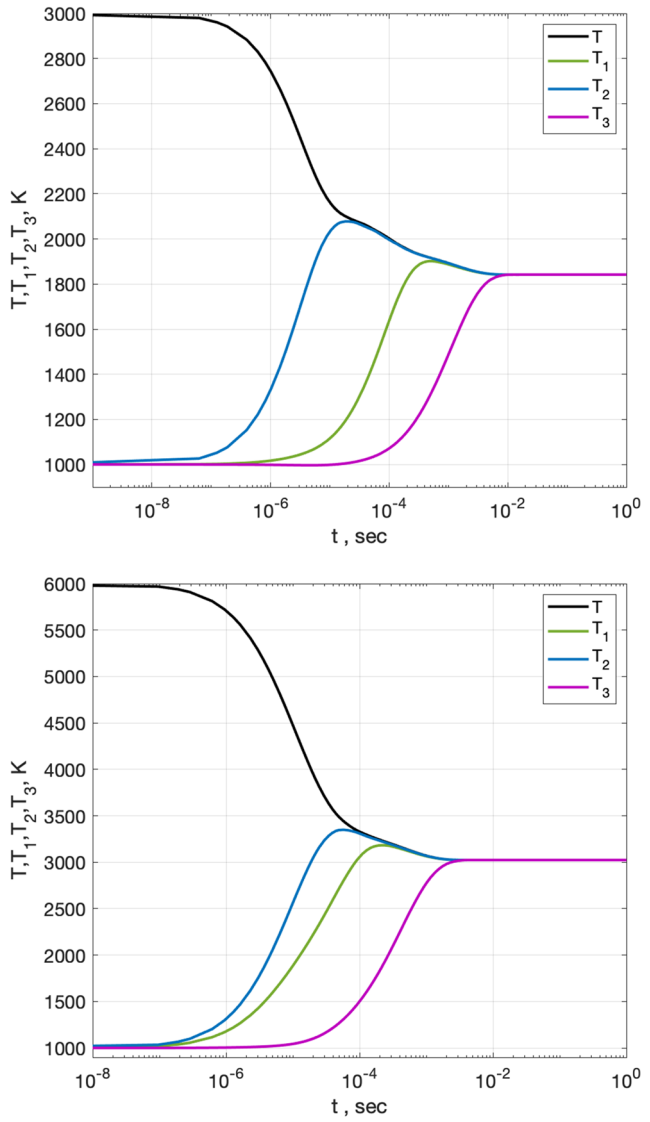

FIG. 3. Evolution of the gas temperature and vibrational temperatures. Anharmonic oscillator model. Initial conditions $p = 100$ Pa, $T^{(0)} = 3000$ K, $T_V^{(0)} = 1000$ K (top panel) and $T^{(0)} = 6000$ K, $T_V^{(0)} = 1000$ K (bottom panel).

For further assessment of the four-temperature model accuracy, we have studied several additional test cases, allowing for the initial excitation of various CO_2 vibrational modes, and compared the data obtained in the 4T and STS approaches for different initial conditions. The initial gas temperature is $T^{(0)} = 3000$ K, and the pressure $p^{(0)} = 100$ Pa. The following initial conditions were considered:

TC1: $T_1^{(0)} = 1000$ K, $T_2^{(0)} = T_3^{(0)} = T^{(0)}$;
TC2: $T_2^{(0)} = 1000$ K, $T_1^{(0)} = T_3^{(0)} = T^{(0)}$;
TC3: $T_3^{(0)} = 1000$ K, $T_1^{(0)} = T_2^{(0)} = T^{(0)}$;
TC4: $T_1^{(0)} = 300$ K, $T_2^{(0)} = 1000$ K, and $T_3^{(0)} = 2000$ K.

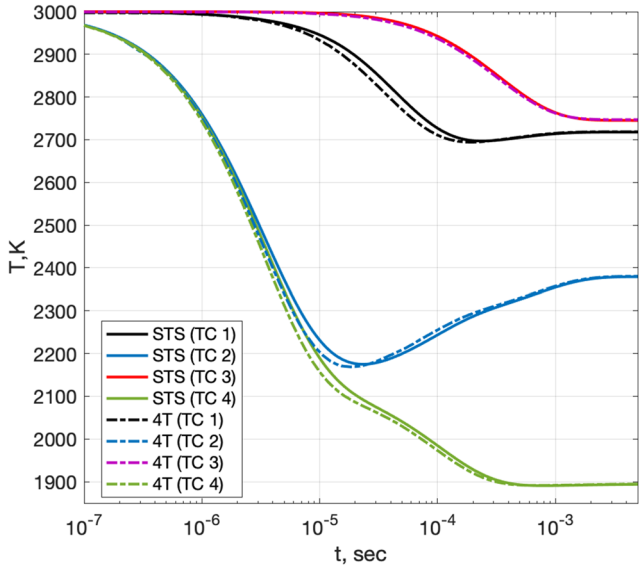

FIG. 4. Evolution of the gas temperature for different test cases. Anharmonic oscillator model.

It is clear that some of those test cases are hypothetical and cannot be observed in real gas flows; however, they are used to check the robustness of the 4T model under arbitrary conditions.

The comparison of the gas temperatures obtained in four-temperature and state-to-state approaches is shown in Fig. 4. For all presented cases, the four-temperature approximation is in excellent agreement with the state-to-state results (differences do not exceed 1.5%). Note that for harmonic oscillators, the coincidence is even better for most cases, and the temperature values diverge by less than 0.4%.

Based on the above analysis, we conclude that the four-temperature model provides a rather accurate and efficient alternative to the state-to-state description of the vibrational relaxation in CO_2. Therefore, we use the 4T model for further assessment of the 3T simulation accuracy. Calculations were performed in the three-temperature and four-temperature approximations for different initial conditions. The initial gas temperatures and vibrational temperatures were varied in the range from 500 K to 5000 K with a step of 500 K.

The discrepancy between the solutions was quantified using the maximum percentage deviation calculated using the following formula:

$$\delta = \frac{\left|T^{(3T)} - T^{(4T)}\right|}{T^{(4T)}} \cdot 100\%.$$

The maximum error was computed for each pair of $T^{(0)}$ and $T_V^{(0)}$.

In Fig. 5, the maximum error between solutions found with the use of various approaches is presented in dependence on initial temperatures $T^{(0)}$, $T_V^{(0)}$. It can be seen that the overall difference is considerably greater between the results obtained with a simplified description of the energy production rates according to the Landau–Teller formula (the maximum difference reaches 70%). The discrepancy between the gas temperatures obtained in

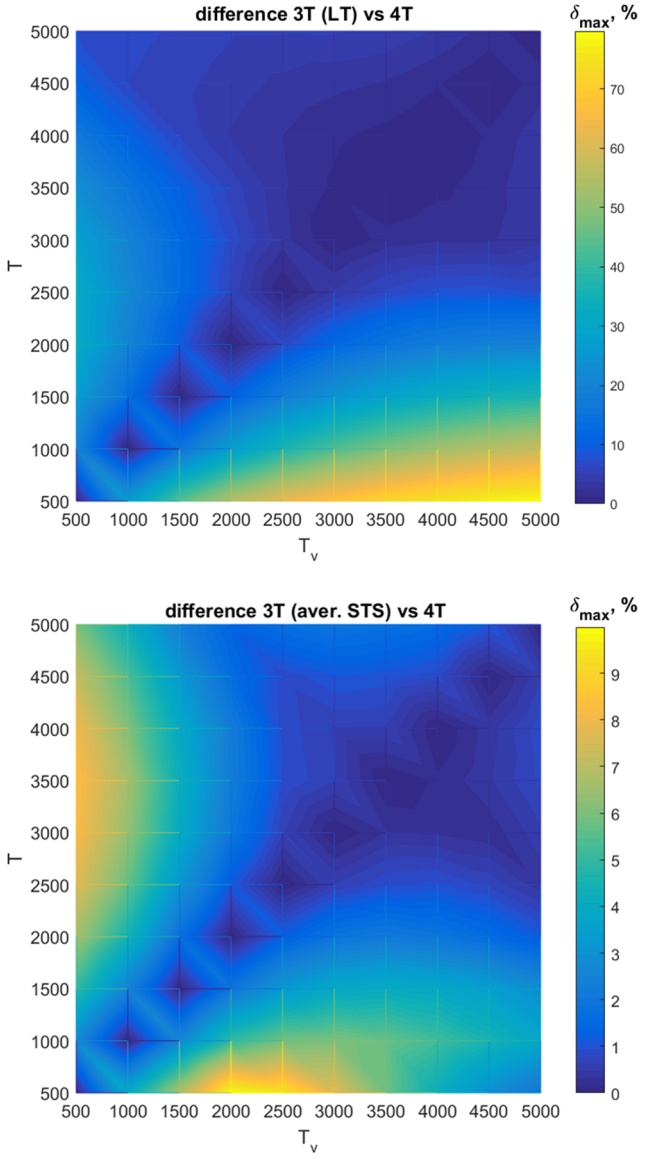

FIG. 5. Maximum relative error for the temperature obtained using the 3T model with respect to the 4T model for different sets of the initial conditions. Landau–Teller formulation (top); averaged STS relaxation terms (bottom).

the four-temperature and three-temperature approaches with the averaged state-to-state relaxation terms occurs much less and does not exceed 10%. The initial vibrational excitation has a noticeable effect on the results obtained in the simplified Landau–Teller formulation: the difference increases with $T_V^{(0)}$ [Fig. 5 (top)]. This effect may occur because relaxation times[36] were measured under shock wave conditions and are not suitable for ratios $T_V/T > 1$. On the other hand, for $T_V < T$, the simplified formulation gives reasonable agreement with four-temperature results, and the deviation between temperature values stays within 30%–35%. It could be mentioned

that using more accurate data on the relaxation times may provide more accurate results while keeping low simulation costs. The problem is that at the present time, no reliable measurements are available for the relaxation times of different CO_2 modes, which can be used for both $T_V/T > 1$ and $T_V/T < 1$.

When comparing the multi-temperature results with averaged state-to-state relaxation terms, it can be seen that the ratio of initial gas temperatures has a major influence [Fig. 5 (bottom)]. In this case, differences between solutions arise due to VT_1 transitions, which are taken into account in the four-temperature description; this process is more important than VV_{1-2} or VT_3, as mentioned in Ref. 23. For instance, the vibrational excitation leads to a sharp increase in the error near the point corresponding to $T^{(0)} = 500$ K, $T_V^{(0)} = 2000$ K; with a further increase in initial temperatures, the difference becomes smaller. The same happens at low $T^{(0)}$ and ratio $T^{(0)}/T^{(0)}$ about 5–7. Such behavior is explained by different relations between characteristic times of processes, which prevail under different conditions. For example, under high-temperature conditions, the major contribution is given by the VT_2 process, which has the same description in four-temperature and three-temperature (with averaged state-to-state relaxation terms) approaches; therefore, the solutions have better agreement.

Finally, it is worth mentioning that under conditions of high initial temperatures (which correspond to the right upper corner of Fig. 5), the differences do not exceed 5%, and the reduced 3T models can be used. However, since in the real gas flows the temperatures may vary from low to high values throughout the flow domain, we recommend using the 4T model, which yields best agreement with the STS one for arbitrary initial conditions.

To assess the 4T model not only in the space-homogeneous problem but also in the gas flow, we have carried out additional simulations. A one-dimensional flow behind the plane shock wave has been studied using both the developed 4T model and the conventional two-temperature model[10] with $T_1 = T_2 = T_3 = T_V$; in the latter case, the Landau–Teller expressions with the relaxation times of Ref. 36 are used. The free stream conditions are $T_0 = T_{V0} = 300$ K, $\rho = 1.1751 \cdot 10^{-4}$ kg/m^3, and Mach number M = 5. In Fig. 6, one can see a considerable difference in the density and temperature distributions obtained in the frame of the two models. For the two-temperature model, there is a noticeable incubation time of vibrational relaxation; however, the overall relaxation is faster. In the 4T model, the relaxation starts earlier due to the efficient VT_2 exchange in the bending mode; the asymmetric mode attains equilibrium slowly, which is in line with other studies.[37] Such discrepancies confirm limitations of the 2T model and the Landau–Teller approach in CO_2 simulations (see also Ref. 41).

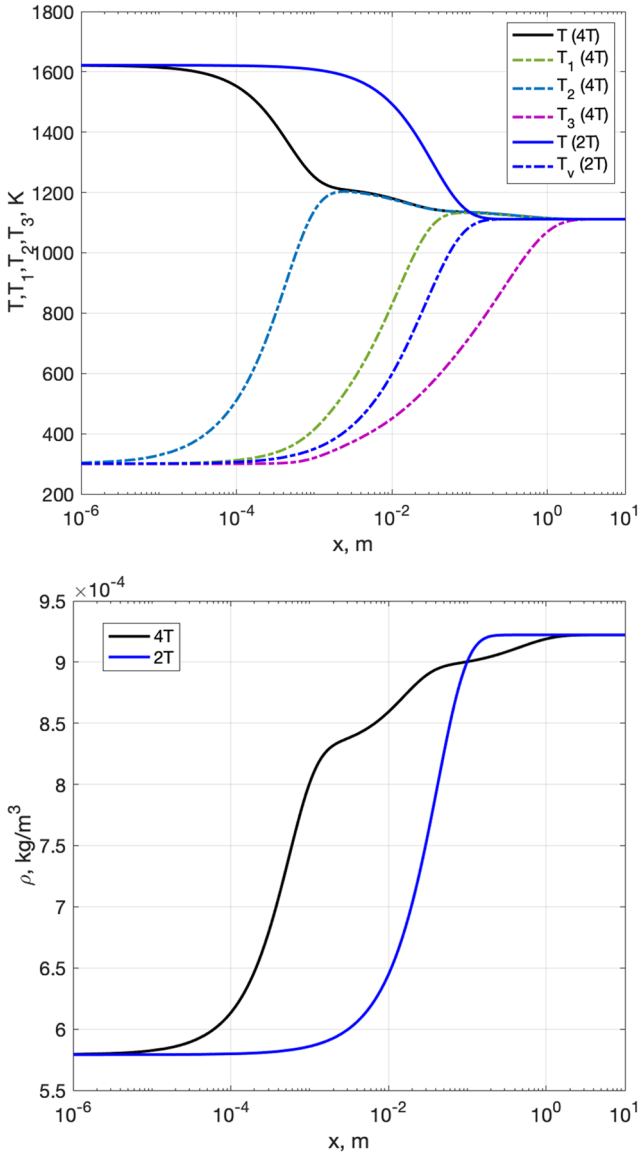

FIG. 6. Evolution of the gas temperature and vibrational temperatures (top panel) and density (bottom panel) behind the shock wave as a function of the distance x from the shock front.

B. Evaluation of numerical efficiency

It is commonly assumed in the CFD that multi-temperature (MT) simulations are much more efficient than the state-to-state (STS) ones. It is clear from the point of view of the number of differential equations solved using the two approaches: a few equations in the MT models vs hundreds and thousands of equations in the STS approach. However, if the MT energy production terms are calculated using the averaged STS relaxation terms, the efficiency of multi-temperature simulations may decrease significantly.

This section provides an estimate of the time spent on solving the problem of 0D vibrational relaxation of pure CO_2 in the frame of three approaches: (1) state-to-state (STS) approximation, (2) four-temperature (4T) approximation using state-averaged relaxation terms, and (3) three-temperature (3T) approximation using the Landau–Teller formulation with relaxation times proposed by Losev *et al.*[36] For comparison, the problem was solved using the Matlab package with a given equal computational accuracy, an integration interval, and the initial conditions. Table I shows the execution time and the total number of calls to the main functions for the numerical solution.

TABLE I. Performance time of functions.

Function	Calls			Total time (s)			Run time (s)		
	STS	4T	3T	STS	4T	3T	STS	4T	3T
`ode15s` (solves stiff ODEs, variable order method)	1	1	1	767.129	559.405	206.293	767.129	559.405	206.293
`rpart` (calculates the RHS of ODEs)	24 668	883	485	318.945	559.157	206.156	0.013	0.633	0.425
`odenumjac` (numerically computes the Jacobian)	3	3	2	338.197	7.721	2.250	112.732	2.574	1.125

The time of numerical integration using the 4T and 3T approaches, respectively, is 27% and 73% less than using the STS one. It is interesting to note that the most time-consuming step for the STS approach is the calculation of the Jacobian of the system, which takes 41% of the total calculation time; in the 4T and 3T approaches, 99.9% of the time is spent on computing the right-hand sides of the considered system. As a result, in terms of time costs, the use of a simple Landau–Teller relation to describe the relaxation process is the most advantageous; this is not surprising since the production terms are computed using analytical approximations for the relaxation times.

One can see that using the STS production rates in the 4T simulations considerably reduces the overall numerical efficiency of the four-temperature model. However, one has to keep in mind that in this study, we consider a 0D problem. In 2D or 3D simulations, the most time-consuming routines are those for the calculation of transport coefficients. Computation of the transport terms requires solving, in each cell of the mesh, linear transport systems containing about N equations (N is the total number of species in a mixture including vibrational states in the STS approach); the coefficients in equations are collision integrals. It is obvious that for CO_2 viscous flow simulations, the STS model including several thousands states is hardly applicable, whereas the 4T model can be easily implemented to the CFD.

Another possible way to improve the efficiency of the 4T model is using machine learning techniques for the computation of the averaged state-resolved relaxation terms. Simple regression methods may help to essentially reduce the computational costs for the energy production rates. In our future work, we plan to implement regression techniques and evaluate the gain in numerical simulation costs.

IV. CONCLUSIONS

A new four-temperature model for the vibrational relaxation of carbon dioxide is developed on the basis of kinetic theory methods. Contrarily to models used in previous studies, the proposed approach takes into account VT transitions in each vibrational mode (and not only in the bending mode) as well as all kinds of intermode vibrational energy exchanges between symmetric, bending, and asymmetric CO_2 modes including the VV_{1-2} transitions, which are commonly assumed fast; separate vibrational temperatures are introduced for each mode. Thus, the set of relaxation mechanisms is extended. Another key feature of the model is using the averaged state-resolved relaxation rates instead of conventional Landau–Teller expressions, suffering of serious limitations under strongly non-equilibrium conditions. The model was implemented in the 0D code for modeling spatially homogeneous vibrational relaxation and also used in the 1D simulations of the flow behind the plane shock wave. A comparison with the state-to-state simulations shows excellent agreement between the 4T and STS solutions. On the other hand, using the three-temperature model with the Landau–Teller production rates leads to the significant loss of accuracy. Therefore, the 4T model extends the range of applicability of multi-temperature approaches and can be recommended as a simple and efficient alternative to the STS flow description.

In addition, the numerical efficiency of various models was assessed. It is shown that using the 4T model in a 0D relaxation problem reduces the computational costs up to 30%, which is not that much advantageous as expected. However, implementation of the 4T model to viscous flow solvers will significantly improve the efficiency due to the gain in the computation of transport coefficients compared to the state-to-state model. Application of machine learning methods for the computation of the averaged state-resolve relaxation rates is also rather promising for the computational cost reduction; this will be assessed in our future studies.

ACKNOWLEDGMENTS

This study was supported by the Russian Science Foundation, Grant No. 19-11-00041.

DATA AVAILABILITY

The data that support the findings of this study are available from the corresponding author upon reasonable request.

REFERENCES

[1]E. V. Kustova and E. A. Nagnibeda, "On a correct description of a multi-temperature dissociating CO_2 flow," Chem. Phys. **321**, 293–310 (2006).
[2]E. Nagnibeda and E. Kustova, *Nonequilibrium Reacting Gas Flows: Kinetic Theory of Transport and Relaxation Processes* (Springer-Verlag, Berlin, Heidelberg, 2009).
[3]I. Armenise and E. V. Kustova, "State-to-state models for CO_2 molecules: From the theory to an application to hypersonic boundary layers," Chem. Phys. **415**, 269–281 (2013).
[4]I. Armenise and E. V. Kustova, "On different contributions to the heat flux and diffusion in non-equilibrium flows," Chem. Phys. **428**, 90–104 (2014).
[5]S. Kosuge and K. Aoki, "Shock-wave structure for a polyatomic gas with large bulk viscosity," Phys. Rev. Fluids **3**, 023401 (2018).
[6]S. N. Dhurandhar and A. Bansal, "Chemical kinetics study in rarefied Martian atmosphere using quantum kinetics model," Phys. Fluids **30**(11), 117104 (2018).
[7]E. Kustova, M. Mekhonoshina, and A. Kosareva, "Relaxation processes in carbon dioxide," Phys. Fluids **31**, 046104 (2019).

[8]A. Sahai, C. O. Johnston, B. Lopez, and M. Panesi, "Flow-radiation coupling in CO_2 hypersonic wakes using reduced-order non-Boltzmann models," Phys. Rev. Fluids **4**, 093401 (2019).
[9]E. V. Kustova and E. A. Nagnibeda, "State-to-state theory of vibrational kinetics and dissociation in three-atomic gases," AIP Conf. Proc. **585**, 620–627 (2001).
[10]R. L. Taylor and S. Bitterman, "Survey of vibrational relaxation data for process important in the CO_2–N_2 laser system," Rev. Mod. Phys. **41**(1), 26 (1969).
[11]J. A. Blauer and G. R. Nickerson, "A survey of vibrational relaxation rate data for processes important to CO_2-N_2-H_2O infrared plume radiation," AIAA Paper No. 74-536, 1974.
[12]M. Bartolomei, F. Pirani, A. Laganà, and A. Lombardi, "A full dimensional grid empowered simulation of the CO_2 + CO_2 processes," J. Comput. Chem. **33**, 1806–1819 (2012).
[13]R. N. Schwartz, Z. I. Slawsky, and K. F. Herzfeld, "Calculation of vibrational relaxation times in gases," J. Chem. Phys. **20**, 1591 (1952).
[14]M. Lino da Silva, J. Vargas, and J. Loureiro, "STELLAR CO_2 v2: A database for vibrationally specific excitation and dissociation rates for carbon dioxide," Technical Report IST–IPFN TR 06–2018, IST, Lisbon, December 2018, ESA Contract No. 4000118059/16/NL/KML/fg Standard Kinetic Models for CO2 Dissociating Flows.
[15]V. I. Gorikhovsky and E. A. Nagnibeda, "Energy exchange rate coefficients in modeling carbon dioxide kinetics: Calculation optimization," Vestn. St. Petersburg Univ., Math. **52**(4), 428–435 (2019).
[16]E. Kustova, A. Savelev, and I. Armenise, "State-resolved dissociation and exchange reactions in CO_2 flows," J. Phys. Chem. A **123**(49), 10529–10542 (2019).
[17]R. Aerts, T. Martens, and A. Bogaerts, "Influence of vibrational states on CO_2 splitting by dielectric barrier discharges," J. Phys. Chem. C **116**, 23257–23273 (2012).
[18]A. Bogaerts, W. Wang, A. Berthelot, and V. Guerra, "Modeling plasma-based CO_2 conversion: Crucial role of the dissociation cross section," Plasma Sources Sci. Technol. **25**(5), 055016 (2016).
[19]L. D. Pietanza, G. Colonna, G. D'Ammando, and M. Capitelli, "Time-dependent coupling of electron energy distribution function, vibrational kinetics of the asymmetric mode of CO_2 and dissociation, ionization and electronic excitation kinetics under discharge and post-discharge conditions," Plasma Phys. Controlled Fusion **59**, 014035 (2017).
[20]T. Silva, M. Grofulović, B. L. M. Klarenaar, A. S. Morillo-Candas, O. Guaitella, R. Engeln, C. D. Pintassilgo, and V. Guerra, "Kinetic study of low-temperature CO_2 plasmas under non-equilibrium conditions. I. Relaxation of vibrational energy," Plasma Sources Sci. Technol. **27**(1), 015019 (2018).
[21]I. Armenise and E. Kustova, "Mechanisms of coupled vibrational relaxation and dissociation in carbon dioxide," J. Phys. Chem. A **122**, 5107–5120 (2018).
[22]I. Armenise, P. Reynier, and E. Kustova, "Advanced models for vibrational and chemical kinetics applied to Mars entry aerothermodynamics," J. Thermophys. Heat Transfer **30**(4), 705–720 (2016).
[23]O. Kunova, A. Kosareva, E. Kustova, and E. Nagnibeda, "Vibrational relaxation of carbon dioxide in various approaches," Phys. Rev. Fluids **5**, 123401 (2020).
[24]L. B. Ibragimova, G. D. Smekhov, O. P. Shatalov, A. V. Eremin, and V. V. Shumova, "Dissociation of CO_2 molecules in a wide temperature range," High Temp. **38**(1), 33–36 (2000).
[25]G. Herzberg, *Infrared and Raman Spectra of Polyatomic Molecules* (D.Van Nostrand Company, Inc., New York, 1951).
[26]M. Grofulović, L. L. Alves, and V. Guerra, "Electron-neutral scattering cross sections for CO_2: A complete and consistent set and an assessment of dissociation," J. Phys. D: Appl. Phys. **49**(39), 395207 (2016).
[27]M. Grofulović, T. Silva, B. L. M. Klarenaar, A. S. Morillo-Candas, O. Guaitella, R. Engeln, C. D. Pintassilgo, and V. Guerra, "Kinetic study of CO_2 plasmas under non-equilibrium conditions. II. Input of vibrational energy," Plasma Sources Sci. Technol. **27**(11), 115009 (2018).
[28]B. R. Hollis and J. N. Perkins, "Hypervelocity aeroheating measurements in wake of Mars mission entry vehicle," AIAA Paper No. 95-2314, 1995.
[29]B. R. Hollis and J. N. Perkins, "High-enthalpy aerothermodynamics of a Mars entry vehicle. Part 1: Experimental results," J. Spacecr. Rockets **34**(4), 449–456 (1997).
[30]H. Takayanagi, A. Lemal, S. Nomura, and K. Fujita, "Measurements of carbon dioxide nonequilibrium infrared radiation in shocked and expanded flows," J. Thermophys. Heat Transfer **32**(2), 483–494 (2018).
[31]C. E. Treanor, J. W. Rich, and R. G. Rehm, "Vibrational relaxation of anharmonic oscillators with exchange dominated collisions," J. Chem. Phys. **48**, 1798 (1968).
[32]E. V. Kustova and E. A. Nagnibeda, "Kinetic model for multi-temperature flows of reacting carbon dioxide mixture," Chem. Phys. **398**, 111–117 (2012).
[33]E. V. Kustova, E. A. Nagnibeda, Y. D. Shevelev, and N. G. Syzranova, "Comparison of different models for non-equilibrium CO2 flows in a shock layer near a blunt body," Shock Waves **21**(3), 273–287 (2011).
[34]A. A. Kosareva and E. A. Nagnibeda, "Vibrational-chemical coupling in mixtures CO_2/CO/O and CO_2/CO/O_2/O/C," J. Phys.: Conf. Ser. **815**(1), 012027 (2017).
[35]A. Kosareva and G. Shoev, "Numerical simulation of a CO_2, CO, O_2, O, C mixture: Validation through comparisons with results obtained in a ground-based facility and thermochemical effects," Acta Astronaut. **160**, 461–478 (2019).
[36]S. Losev, P. Kozlov, L. Kuznezova, V. Makarov, Y. Romanenko, S. Surzhikov, and G. Zalogin, "Radiation of CO_2-N_2-Ar mixture in a shock wave: Experiment and modeling," in *Proceedings of 3rd European Symposium on Aerothermodynamics for Space Vehicles* (ESTEC, Noordwiik, 1998), Vol. 426, pp. 437–444.
[37]Q. Binauld, P. Rivière, J.-M. Lamet, L. Tessé, and A. Soufiani, "CO_2 IR radiation modelling with a multi-temperature approach in flows under vibrational nonequilibrium," J. Quant. Spectrosc. Radiat. Transfer **239**, 106652 (2019).
[38]E. Kustova, E. Nagnibeda, G. Oblapenko, A. Savelev, and I. Sharafutdinov, "Advanced models for vibrational-chemical coupling in multi-temperature flows," Chem. Phys. **464**, 1–13 (2016).
[39]I. N. Kadochnikov, B. I. Loukhovitski, and A. M. Starik, "A modified model of mode approximation for nitrogen plasma based on the state-to-state approach," Plasma Sources Sci. Technol. **24**(5), 055008 (2015).
[40]B. Gordiets, A. Osipov, and L. Shelepin, *Kinetic Processes in Gases and Molecular Lasers* (Nauka, Moscow, 1980).
[41]E. Kustova and M. Mekhonoshina, "Multi-temperature vibrational energy relaxation rates in CO_2," Phys. Fluids **32**, 096101 (2020).